Selectively dissolving CO_2 in highly fluorinated non-porous crystalline materials

Iñigo J. Vitórica-Yrezábal,[1,2†]* Craig A. McAnally,[3] Ashleigh J. Fletcher,[3] Mark R. Warren,[4] Adrian H. Hill,[5‡] Stephen P. Thompson,[4] Martin Quinn,[2] Sam Mottley,[2] Stephen Mottley,[2] Lee Brammer[1]*

1. Department of Chemistry, University of Sheffield, Sheffield S3 7HF, UK.
2. School of Natural Science, University of Manchester, Oxford Road, Manchester, M13 9PL, UK.
3. Department of Chemical and Process Engineering, University of Strathclyde, 75 Montrose St, Glasgow G1 1XJ, Scotland.
4. Diamond Light Source, Harwell Science and Innovation Campus, Didcot, Oxfordshire OX11 0DE, UK
5. ESRF - The European Synchrotron Radiation Facility, 71 Av. des Martyrs, 38000 Grenoble, France

ABSTRACT

Separation of CO_2 from gas mixtures is important is specific applications such as purification of CH_4 gas and blue hydrogen production and more generally in the separation and processing of greenhouse effect gases to mitigate the hazardous effects of global warming. Herein, we report the selective CO_2 sorption by a family of isoreticular, flexible silver coordination polymers (AgCPs) that are ostensibly non-porous but exhibit latent porosity to CO_2 above a gate pressure, through a mechanism akin to dissolution in fluoroalkanes. The CO_2 sorption properties are rationally modified by changing the length of the perfluorocarboxylate ligands. The AgCPs show an absence of CH_4 adsorption due to the lack of pores and channels in their structure and the failure of the dissolution mechanism due to alkane-perfluoroalkane immiscibility. *In situ* single-crystal and powder X-ray diffraction enable the direct visualization of the binding domains of adsorbed CO_2 molecules as well as the associated structural changes of the AgCPs and confirming the gating of CO_2 uptake. The deployment of perfluoroalkylcarboxylate ligands combined with the flexibility of the silver(I) coordination sphere to generate highly fluorinated but mobile regions of the crystals plays an integral role in the selective sorption of CO_2 over CH_4.

INTRODUCTION

The design and synthesis of new materials for applications in molecular separations has received increasing attention in the past two decades.[1-2] In particular, materials able to selectively separate mixtures of industrial relevance have been investigated since most manufactured chemical products are obtained as a combination of products that require further purification steps.[3] Separation and purification often relies on energy-intense methods such as distillation, crystallization, chemisorption (amine scrubbers for CO_2) or evaporation, processes which account for 10-15% of the global energy consumption.[4] With predictions of a three-fold increase in energy demand by 2050,[5] new more-efficient purification materials and technologies are required. In this context, porous materials such as zeolites[6] activated carbon[7] and covalent organic frameworks (COFs)[8] have been extensively studied as adsorbents. Due to their modularity and amenability to design, however, coordination polymers (CPs) and metal-organic frameworks (MOFs) present the broadest scope for design and tunability as energy-efficient physisorbents to store and separate molecules.[9] These crystalline porous materials have been classified as belonging to 1st to 4th generations based on evolution of their structural features and dynamic response to stimuli:[10] 1st generation MOFs are able to accommodate guest molecules, but lose their structural integrity upon guest removal; 2nd generation MOFs retain their structures upon guest insertion/removal, exhibiting permanent porosity; 3rd generation MOFs, also known as flexible or soft MOFs, show reversible structural transformations upon exposure to external stimuli; and 4th generation materials are able to modify their pore size and chemistry, having self-switching pores under the influence of an external stimulus. Although 1st and 2nd generation MOFs are well established, 3rd and 4th generation flexible MOFs remain uncommon due to the challenges involving the design, synthesis and the identification of dynamic behaviour in such materials. Second-generation MOFs typically exhibit Type I adsorption

isotherms (Figure 1a), where the gas sorption/desorption processes often take place at low gas pressures and may lie outside the operationally relevant range for industrial plants, thus decreasing their working capacity.[11,12] Third and fourth-generation MOFs have desirable F-type sorption profiles (Figures 1b-d) as a consequence of the structural transformations incurred during the sorption process.[13,14]

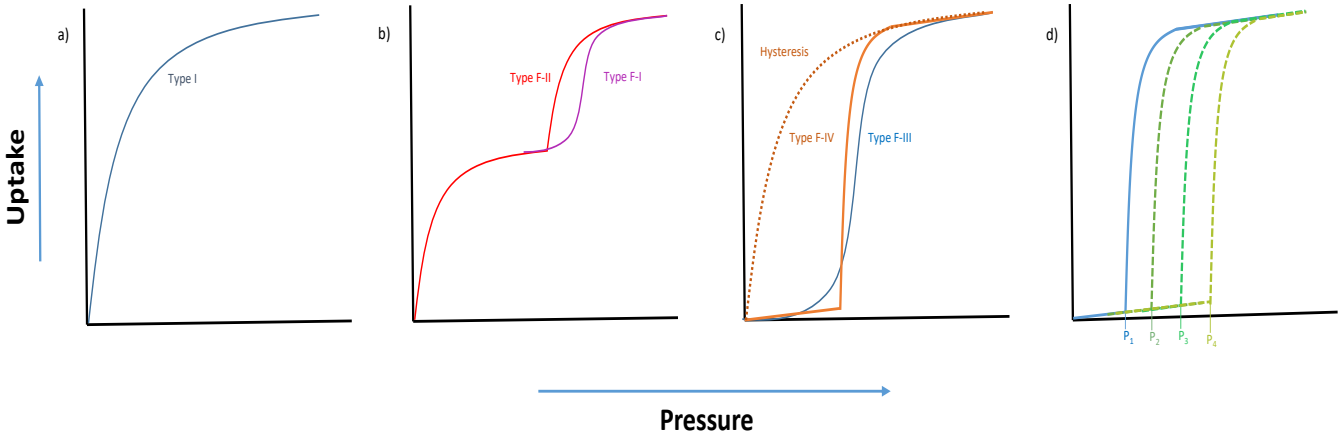

Figure 1. Schematic representation of the gas uptake corresponding to (**a)** a Type I isotherm typical of a rigid 2nd generation MOF; (**b)** Type F-I (gradual in purple) and F-II (abrupt in red) isotherms, typical of a flexible 3rd generation MOF involved in a transformation from open to more open; (**c)** Type F-III (gradual, blue) and F-IV (abrupt, orange) isotherms and hysteresis in the desorption process (orange dotted) typical of a flexible 4th generation MOF. (**d)** Type F-IV isotherms typical of a 4th generation MOFs in which rational modification of the structure induces a gradual change in the gate-pressure threshold.[13]

4th generation materials typically exhibit a stepped sorption profile, which arises from the structural conversion between closed-pore and open-pore forms. A distinctive pressure threshold for switching (gate pressure) also characterizes the sorption profile, below which the material exhibits negligible gas sorption. Such flexible materials represent a potential solution to gas storage, offering higher working capacities for the more volatile gases (O_2, H_2, CH_4 or C_2H_2) for which high-pressure storage is not feasible.[11] The gas separation properties of 4th generation CPs/MOFs remains underexplored due to the novelty and rarity of these materials.[15] Nevertheless, these materials are attracting attention as their stepped adsorption profiles can provide high adsorption selectivity.[11,14] This is especially relevant when only a single gas in a mixture induces the structural transformation that enables sorption.

Previously, we have reported the synthesis of crystalline one-dimensional silver coordination polymers (AgCPs), $[Ag_4(O_2C(CF_2)_mCF_3)_4(TMP)_3]$ (m = 2 (**1**) and 3 (**2**), TMP = 2,3,5,6 tetramethylpyrazine), the crystal structures of which lack defined voids or channels normally associated with porosity.[16-18] Crystals of **1** and **2** reversibly react with small alcohol vapours without losing crystal integrity. This process involves the insertion of alcohol molecules into a metal-carboxylate (Ag−O) bond, accompanied by the formation of an O−H···O hydrogen bond between the coordinated alcohol molecule and the pendant carbonyl group of the now monodentate carboxylate (Figure S10). Our studies suggested that mobility of the perfluoroalkyl groups enables transport of small molecule guests via transient voids within the crystals.[16-18] Building upon this foundation, herein we describe the CO_2 and CH_4 gas adsorption properties and associated structural transformations of the homologous series of five non-porous isoreticular AgCPs $[Ag_4(O_2C(CF_2)_mCF_3)_4(TMP)_3]$ (m = 2 (**1**), 3 (**2**), 4 (**3**), 5 (**4**) and 6 (**5**)). We show that these materials enable adsorption, transport and encapsulation of CO_2 molecules in a process akin to dissolution in liquids, but occurring only above gate pressures that are dependent upon the length of the perfluoroalkyl groups of the carboxylate ligands (Figures 1d and 3a). By contrast, CH_4 adsorption is prevented, enabling excellent CO_2/CH_4 separation characteristics.

RESULTS AND DISCUSSION

Synthesis and crystal structure of AgCPs 1-5. A homologous series of isoreticular AgCPs $[Ag_4(CO_2(CF_2)_mCF_3)_4(TMP)_3(ROH)_2]\cdot xCH_2Cl_2$ (m = 2 (**1-MeOH**), 3 (**2-EtOH**), 4 (**3-EtOH**), 5 (**4-MeOH**) and 6 (**5-MeOH**); ROH = methanol or ethanol; x = 0 or 1(**5-MeOH** only)) has been synthesized as large colourless needle crystals by slow diffusion of a dichloromethane solution of 2,3,5,6-tetramethylpyrazine (TMP) into an alcoholic solution of $Ag(CO_2(CF_2)_mCF_3)$ (m = 2, 3, 4, 5 or 6) at 278 K. Alcohol-free AgCPs $[Ag_4(CO_2(CF_2)_mCF_3)_4(TMP)_3]$ (m = 2 (**1**), 3 (**2**), 4 (**3**), 5 (**4**) and 6 (**5**)) were obtained upon mild heating of the alcohol-containing materials **1-5-ROH** (details in SI sections S1 and S3.1-2). The crystal structures of AgCPs **1-5** comprise pairs of silver(I) ions bridged by pairs of perfluorocarboxylate ligands forming di-silver units $Ag_2(O_2C(CF_2)_mCF_3)_2$, which are linked by pairs of TMP ligands resulting in $Ag_4(O_2C(CF_2)_mCF_3)_4(TMP)_2$ units (m =2-6). These tetramer units are further linked by single-ligand TMP bridges to form a polymeric zig-zag tape (**1-5**). The individual polymers assemble in a rod-like distorted hexagonal packing motif wherein the fluoroalkyl groups project orthogonal to the AgCP tape direction and form fluoroalkyl layers through interdigitation with neighbouring polymers (Figures 2 and S11-S21). The fluoroalkyl groups exhibit some disorder in the crystal structures, suggesting some inefficiency in packing and a degree of mobility as a consequence of the weak dispersion interactions between them.[19,20] The fluoroalkyl moieties adopt either a straight or bent overall configuration as a consequence of either *gauche* or *anti* conformations around the C_n-C_{n+1} (n = 2-4) bonds. Alcohol-free AgCPs **1** ($\mathbf{1_A^{HT}}$, $\mathbf{1_A^{LT}}$, $\mathbf{1_B^{HT}}$ and $\mathbf{1_B^{LT}}$), **2** ($\mathbf{2^{HT}}$ and $\mathbf{2^{LT}}$) and **3** ($\mathbf{3^{HT}}$ and $\mathbf{3^{LT}}$) have high-temperature (HT) and low-temperature (LT) polymorphs, which differ in the conformation of the fluoroalkyl groups(*anti*/*gauche*), requiring a reduction in crystallographic symmetry for LT forms of **1-3**. Additionally, polymorphs of coordination polymer **1** can be further subdivided into two classifications (A or B) depending on the relative arrangement of neighbouring 1D coordination polymer tapes.[18] The polymorphism in coordination polymers **1-3** arises from the conformational flexibility shown in the fluoroalkyl groups and the orientation of the single-bridge TMP ligand relative to the $Ag_4(O_2C(CF_2)_mCF_3)_4(TMP)_2$ (m = 2, 3, 4, 5, 6) units.

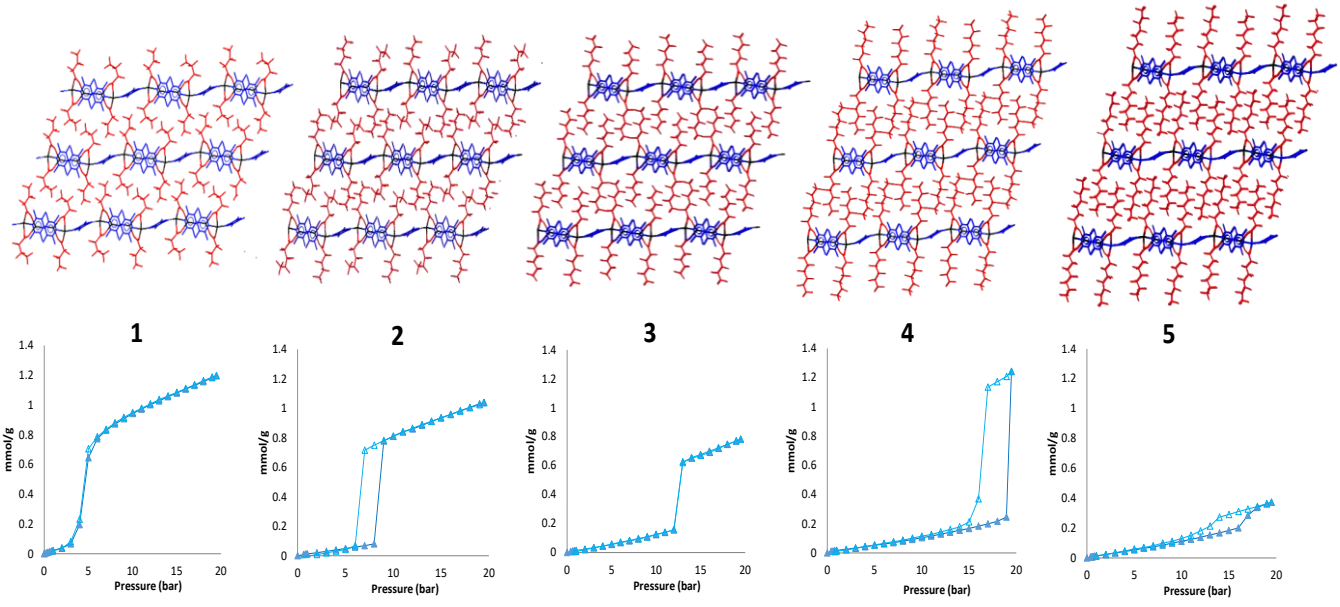

Figure 2. *Top:* Crystal structures of AgCPs **1-5,** showing polymeric zigzag tapes extending horizontally via alternating single and double TMP bridges between pairs of Ag(I) centres. Interdigitation of perfluoroalkyl groups creates fluoroalkyl regions between the coordination polymers. Perfluorocarboxylates shown in red, TMP ligands in blue and silver atoms in black. *Bottom:* CO_2 adsorption isotherms at 273 K for AgCPs **1-5**, solid triangles represent adsorption and open triangles represent desorption.

CO_2 and CH_4 sorption by AgCPs 1-5. CO_2 adsorption isotherms were measured for AgCPs **1-5** at 273 K (Figure 2). These Type F-III (for **1** and **5**) and F-IV (for **2-4**) adsorption isotherms illustrate that the gas

uptake is gated and diffraction studies show the gate is accompanied by a structural change from non-porous to guest-containing structure (*vide infra*). There is a monotonic trend of increasing gate pressure with increasing perfluoroalkyl chain length (Figure 3a,b) with gate opening pressures of approx. 3 bar for **1**, 8 bar for **2**, 12 bar for **3**, 19 bar for **4**. Coordination polymer **5** does not appear to continue this trend within our experimentally accessible pressure range ($p \leq 19.5$ bar; $p/p_0 \leq 0.54$ at 273 K) for the isotherm measurements and exhibits a gate at 16 bar, although involving a much smaller adsorption step than those for **1**-**4**. This smaller lower-pressure step for **5** could also represent a small initial gate-opening that precedes a larger, higher-pressure step (i.e., $p > 19.5$ bar) more comparable to the gating processes observed for **1**-**4**, a supposition supported by *in situ* PXRD studies (*vide infra*).

Maximum CO_2 adsorption capacities (19.5 bar, 273 K, Figure 2) revealed the uptake of 2.0 CO_2 molecules/formula unit (FU) for **1** (1.19 mmol g^{-1}) and **2** (1.03 mmol g^{-1}), 1.6 CO_2 molecules/FU for **3** (0.78 mmol g^{-1}), 2.8 CO_2 molecules/FU for **4** (1.24 mmol g^{-1}) and only 0.9 CO_2 molecules/FU for **5** (0.37 mmol g^{-1}). Overall interpretation of the trend in adsorption will be considered through combination of these results with crystallographic studies (Figure 3c, *vide infra*). The CO_2 isotherms for **4** and **5** were also measured at 263 K for comparison and show modest increases in adsorption capacity relative to 273 K (Figures S120-S125). Interestingly, the isotherm for **4** now exhibits three separate adsorption steps with onsets at pressures of 14, 16 and 18 bar CO_2 (Figure S121), corresponding to adsorption of approximately one CO_2 molecule/FU at each step, suggesting, as implied by the study of **5**, that adsorption of CO_2 in these perfluoroalkylated materials can be a multi-step process, dependent upon perfluoroalkyl chain length and upon adsorption conditions (T, p).

CH_4 adsorption isotherms measured for AgCPs **1** and **2** at 273 K (Figures S126, S127) are a marked contrast to the CO_2 isotherms. These Type III isotherms, characteristic of nonporous materials, confirm negligible CH_4 adsorption by **1** and **2** in the pressure range evaluated.

CO_2 and CH_4 gas sorption studied by X-ray diffraction. In order to explore structural changes associated with the CO_2 gas uptake by CPs **1**-**5**, *in situ* synchrotron PXRD measurements at room temperature were made at sequential gas pressures up to 50 bar (SI section S4) using a gas cell/rig configuration at beamlines ID31 (ESRF)[21] and I11 (Diamond Light Source). Initial measurements under vacuum enabled characterization of previously established forms[16-18] of **1** (polymorph $\mathbf{1_B^{HT}}$), **2** (polymorph $\mathbf{2^{LT}}$), **4** and **5** by Pawley fitting of the patterns.[22] Data for AgCP **3** suggested a new, unknown polymorph and prevented further analysis of this material. In each case a series of PXRD patterns were obtained after equilibration at different gas pressures. Pawley fitting of these patterns allowed unit cell parameters to be determined (Tables S12, S15-S17), and established that gated increases in volume per formula unit (V/Z) occur in all cases, sometimes accompanied by changes in translational symmetry, but consistent with adsorption of CO_2.

Adsorption behaviour might be expected to resemble that documented by gravimetric adsorption measurements, but not match exactly as conditions (T, p) are different. Volume increases ($\Delta V/Z$) provide estimates of CO_2 adsorption,[23-25] immediately after the gate opening pressures (Figure 3c), of 0.75-0.94 CO_2/FU for **1** (gate at $4.2 < p < 9.8$ bar), 1.23-1.39 CO_2/FU for **2** (gate at $17.6 < p < 19.1$ bar) and 1.93-2.41 CO_2/FU for **4** (gate at $24.4 < p < 30.0$ bar). The implied trend is one of increasing adsorption (CO_2/FU) and increasing gate pressure with increasing perfluoroalkyl chain length. Gate pressures are higher than observed for gravimetric measurements at 273 K (or 263 K) but accord well based upon relative pressures (p/p_0: 0.08 at 273 K vs 0.07-0.17 at 298 K for **1**; 0.22 at 273 K vs 0.30-0.32 at 298 K for **2**; 0.47-0.60 at 263 K vs 0.54 at 273 K vs 0.42-0.51 at 298 K for **4**). PXRD studies of **5** indicate only small volume increase ($\Delta V/Z$) at $p <$ 48.4 bar (estimated uptake 0.32-0.40 CO_2/FU) at which point a high-pressure gating occurs leading to a larger change in volume (estimated overall uptake 3.38-4.23 CO_2/FU). This behaviour is consistent with that observed in gravimetric adsorption measurements for **5**, which were limited to $p < 19.5$ bar, but suggests greater capacity is accessible at higher pressures.

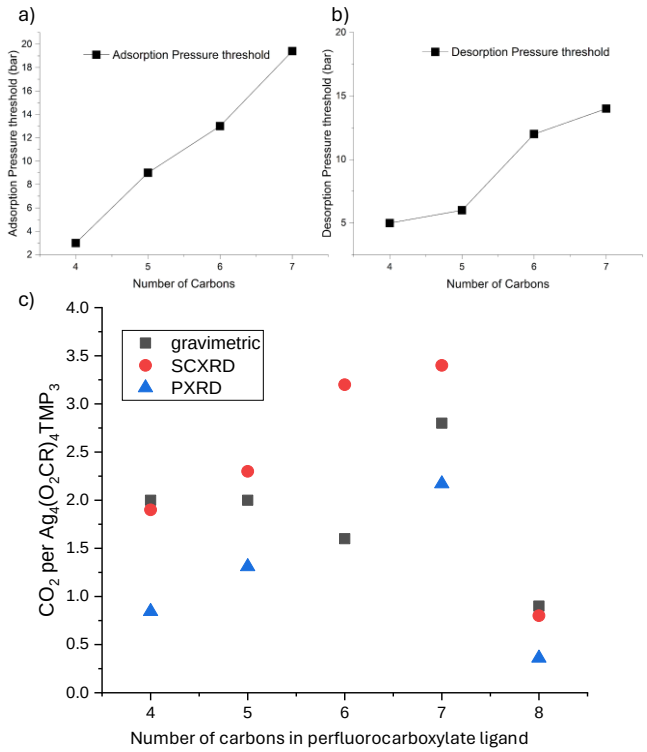

Figure 3. CO_2 pressure threshold at which (a) adsorption and (b) desorption is observed, plotted versus the number of carbons in the perfluorocarboxylate ligands for **1-4**. (c) Number of CO_2 molecules per AgCP formula unit estimated from gravimetric sorption (black squares), from refined CO_2 molecule occupancy from SCXRD (red circles) and from volume increase at initial gate opening from PXRD (blue triangles). Data are plotted versus number of carbons of the perfluorocarboxylate ligands of **1-5**.

Synchrotron PXRD studies (at beamline ID31, ESRF) were also used to identify any structural changes in response to CH_4 uptake for **1** and **5**, both at room temperature and at 180 K. No significant changes in unit cell parameters were observed in the pressure range 1-25 bar for **1** (1-18 bar for **5**). The absence of structural changes suggests that CH_4 is not adsorbed by AgCPs **1** and **5**, consistent with gravimetric adsorption measurements.

To complement the gravimetric adsorption and PXRD studies, and seeking to provide more detailed information on the mechanism and binding sites for CO_2 adsorption, we have undertaken a series of single-crystal X-ray diffraction (SCXRD) studies of **1-5** under a CO_2 atmosphere. Studies were conducted using a gas cell/rig configuration (SI Section S2) with a Rigaku FR-X rotating anode X-ray diffractometer and at I19 beamline at Diamond Light Source synchrotron.[26] A strategy different to that of the PXRD studies was adopted. After initial measurements under vacuum, a sequence of SCXRD studies with full crystal structure determination were conducted under a 10 bar CO_2 atmosphere at temperatures beginning at room temperature and ending at 200 K (232 K for **1**) (SI section S3). This approach increases the relative pressure (p/p_0) of CO_2 while also reducing the thermal motion of the AgCP host and the CO_2 molecules and has allowed crystallographic location of the adsorbed CO_2 molecules and an estimate of the amounts adsorbed (SI section S3.3, Figures S23-S34). The guest-containing AgCPs $\mathbf{1}^{\mathbf{CO2}}$-$\mathbf{4}^{\mathbf{CO2}}$ at the lowest temperatures

studied show a trend of increasing amount of CO_2 molecules/FU (1.9, $\mathbf{1}^{CO2}$; 2.3, $\mathbf{2}^{CO2}$; 3.2, $\mathbf{3}^{CO2}$ and 3.4, $\mathbf{4}^{CO2}$) distributed across 3 sites ($\mathbf{1}^{CO2}$) or 4 sites ($\mathbf{2}^{CO2}$-$\mathbf{4}^{CO2}$) per FU based upon refined occupancies for crystallographically located CO_2 molecules (Figure 3c). The structure of $\mathbf{5}^{CO2}$, however, exhibits much lower uptake (0.8 CO_2 molecules/FU located at a single site). These observations are consistent with the PXRD studies and differ only from the gravimetric adsorption studies in that the overall adsorption of CO_2 appears to be slightly underestimated. The amounts of adsorbed CO_2 determined by the three methods are of similar magnitude, especially given the different approaches taken in their determination, and therefore suggest a consistent behaviour.

The crystal structures of the guest-containing AgCPs $\mathbf{1}^{CO2}$-$\mathbf{5}^{CO2}$ show two distinctive regions where CO_2 gas molecules are located (Figure 4). Sites in the first region lies close to the single-bridge TMP ligands, although some interaction with proximate CF_2 groups is often present, while sites in the second region are better classified as being predominantly associated with the interdigitated perfluoroalkyl ligands. Gated uptake of CO_2 is again evident as initial reduction in temperature resulted in a contraction in volume (*V*/*Z*), suggesting little or no CO_2 uptake, until a temperature was reached at which gate opening occurs, resulting in

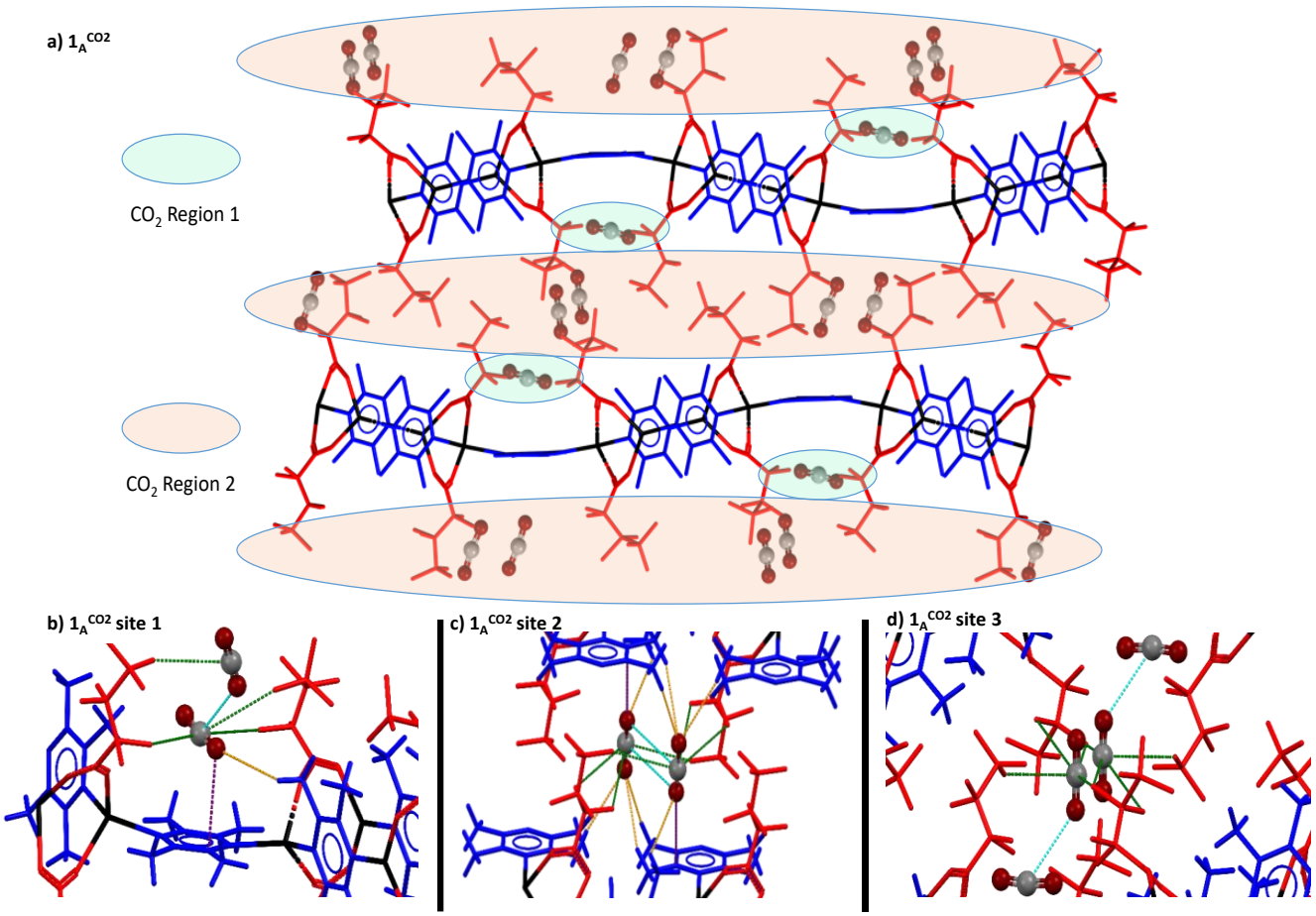

Figure 4. Crystal structure of coordination polymer $\mathbf{1}_A^{CO2}$ at 232 K and 10 bar CO_2, showing (a) the adsorbed CO_2 molecules in region 1 (green) and region 2 (light orange). Specific CO_2 intermolecular interactions are shown: (b) at site 1 (central) with neighbouring site 3 (peripheral), (c) at site 2, which contains an inversion-related pair of CO_2 molecules, and (d) at site 3, which also contains a single CO_2 molecule (central) disordered over an inversion centre (both components shown) and interacting with CO_2 molecules in neighbouring site 1 (peripheral). Colours as in Figure 2 with CO_2 oxygen in dark red and carbon in grey, $CO_2\cdots\pi$ (TMP) shown as purple dashed lines, $CO_2\cdots CH_3$(TMP) C−H···O hydrogen bonds as orange dashed lines, C−F···CO_2 interactions as green dashed lines and $CO_2\cdots CO_2$ interactions in light blue. See Figures S25-S34 for analogous depiction of CO_2 sites for AgCPs **2**-**5**.

an increase in volume and allowing CO_2 molecule(s) to be modelled crystallographically ($\mathbf{1}^{CO2}$, 253K; $\mathbf{2}^{CO2}$, 215 K; $\mathbf{3}^{CO2}$, 230 K; $\mathbf{4}^{CO2}$, 240 K). Given the very different SCXRD approach (*i.e.* isobaric rather than

isothermal), quantitative comparisons with gating behaviour observed from the gravimetric adsorption and PXRD studies cannot be made, but it is important to recognize that the gating observed across all experiments demonstrates a qualitative consistency and provides an assurance of the behaviour. For $\mathbf{5}^{\mathbf{CO2}}$, a temperature of 200 K was required before CO_2 could be modelled, but there was no clear evidence of a volume increase as presumably any such increase (for the much smaller CO_2 uptake) is more than offset by the volume contraction upon cooling.

In all cases ($\mathbf{1}^{\mathbf{CO2}}$-$\mathbf{5}^{\mathbf{CO2}}$), CO_2 preferentially populates the sites in region 1 first, with increasing population of the sites in region 2 observed as the temperature is decreased, forming a number of short interactions with neighbouring atoms of the AgCPs (Figures S24, S26, S29, S30, S32 ,S34). CO_2 molecules in region 1 form C−H···O hydrogen bonds (with the methyl groups of adjacent TMP ligands), CO_2···TMP interactions (parallel $\pi_{CO2}\cdots\pi_{N\text{-}C}$ and T-shaped $O{=}C{=}O^{\delta-}\cdots\pi_{N\text{-}C}$), offset antiparallel (CO···CO) dimers with carboxylate groups and CF_2···CO_2 interactions. The $\pi_{CO2}\cdots\pi_{N\text{-}C}$ interaction between CO_2 and aromatic rings has been previously reported by several groups,[27] and has been described as a mixture between π-π dispersive forces and an electrostatic interaction between the electronegative aromatic π-cloud and the electropositive carbon on the CO_2. The $O{=}C{=}O^{\delta-}\cdots\pi_{N\text{-}C}$ TMP interaction involves electron-poor regions of the conjugated ring, resembling that of anion-π interactions,[28] whereas the CO···CO offset dimers resemble those reported for organic carbonyl groups[29] and for self-interactions between pairs of CO_2 molecules.[30] CO_2 molecules in region 2 also form $O{=}C{=}O^{\delta-}\cdots\pi_{N\text{-}C}$ interactions with TMP ligands but predominantly form CF_2···CO_2 interactions. The latter can be described as electrostatic wherein the fluorides interact with the electropositive carbon of the CO_2 (i.e. $C{-}F^{\delta-}\cdots C^{\delta+}$), although the nature of this interaction has been debated for years, particularly in the context of explaining the high solubility of CO_2 in perfluoroalkanes.[31]

The crystal structures also reveal that the one-dimensional AgCPs **1**-**5** have to rearrange their structure to accommodate the CO_2 guest molecules. Not only are the single-bridge TMP ligands able to reorient by rotation about the longitudinal N···N vector, but the flexible coordination geometry readily accessible by the d^{10} Ag(I) ions allows the single-bridging TMP ligands to pivot around the silver centres, generating pockets of space where CO_2 molecules are accommodated (see SI, Section 3.3 for full descriptions). Such structural also flexibility enables the formation of several polymorphs for AgCPs **1**-**3** and $\mathbf{3}^{\mathbf{CO2}}$ (conversion between $\mathbf{3_A}^{\mathbf{CO2}}$ and $\mathbf{3_B}^{\mathbf{CO2}}$) through end-to-end rotation of the TMP ligand. Indeed, we have previously exploited this process upon more extensive heating to enable loss of the single-bridge TMP ligand (for AgCPs **1** and **2**) to enable a cross-linking solid-state pathway to new 2D AgCPs. [16-18]

Dissolving CO_2 and CO_2/CH_4 separation. The combination of gravimetric adsorption data and diffraction studies has demonstrated the gated CO_2 adsorption by the highly fluorinated, nominally non-porous AgCPs **1**-**5**, in contrast to the absence of significant CH_4 adsorption (established in studies of **1**, **2** and **5**). These observations led us to explore directly the potential for separation of CO_2 from CH_4 by the AgCP materials. Compounds **1** and **2** were selected to explore this potential through measurement of adsorption isotherms of 80/20 and 90/10 CO_2/CH_4 gas mixtures for **1** and **2**, respectively. A total pressure range of $0 < p < 10$ bar at 273 K was used to ensure that the gate pressures determined for the single-component CO_2 adsorption isotherms were exceeded by the partial pressure of CO_2 employed. When plotted as a function of CO2 partial pressure (Figure 5), the CO2/CH4 mixed gas isotherms are very similar to the single component CO2 isotherms, showing gated adsorption at similar gate pressures and the same overall adsorption capacities. This confirms that AgCPs **1** and **2** preferentially adsorb CO2 over CH4 with a selectivity close to 100% in the pressure range measured.

It is envisaged that the interdigitated, but mobile, perfluoroalkyl layers present in these materials (Figure 2) provide a pathway for incursion and thus adsorption of CO_2 by the AgCPs. This is consistent with our observations for incursion of other small molecules by **1**[17,18] and by the observation of conformational flexibility of the perfluoroalkyl chains that leads to polymorphism in these materials as well as enabling (transient) cavities to accommodate and transport CO_2 molecules. The orientational flexibility of the single-

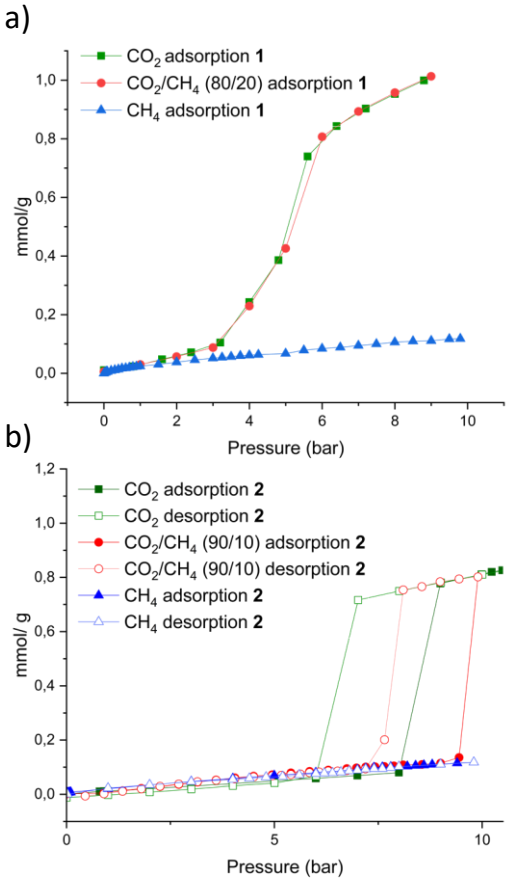

Figure 5. CH_4, CO_2, and CO_2/CH_4 mixtures adsorption/desorption isotherms for AgCPs a) **1** and b) **2**; Red circles for CO_2/CH_4 competitive data for CPs **1** (80/20) and **2** (90/10). Green squares for CO_2 adsorption/desorption for **1** (a) and **2** (b). Blue triangles for CH_4 adsorption/desorption for **1** (a) and **2** (b).

bridge TMP ligands, facilitated by the ease of deformation of the Ag(I) coordination environments, plays an important role in providing CO_2 binding sites in region 1, but $CF_2\cdots CO_2$ interactions are evident in CO_2 binding sites in both region 1 and region 2, and are most prevalent in the latter. Interactions between fluorine atoms and CO_2 molecules have been exploited previously to enhance CO_2 uptake in porous molecular materials[32] and most notably in metal-organic frameworks, such as the SIFSIX[33] and TIFSIX[34] series of MOFs (and related materials) in which the frameworks are pillared by SiF_6^{2-}, TiF_6^{2-} or related fluoroanions and project fluorine atoms into open pores enabling binding of CO_2 molecules by, for example, $Si{-}F^{\delta-}\cdots C^{\delta+}$ interactions. The greater polarity of the Si–F (or Ti–F) bonds will enable a stronger interaction than is suggested herein for $C{-}F^{\delta-}\cdots C^{\delta+}$. Fluorinated organic ligands within MOFs have also been explored,[35-44] predominantly involving fluorinated aromatic linker ligands, including the observation of $C_{Ar}{-}F^{\delta-}\cdots C^{\delta+}$ interactions. More generally the exploitation of fluorinated components in MOFs has recently been reviewed.[41] More closely related to the present study are examples of post-synthetic attachment of perfluoroalkylcarboxylates to the Zr_6 nodes of the MOF NU-1000, DUT-67 and MOF-808.[42-44] The perfluoroalkyl chains project into the cavities of the MOFs and are found to improve water stability (DUT-67) and enhance CO_2 uptake and CO_2 adsorption relative to N_2 adsorption (NU-1000) and relative to CH_4 (MOF-808). Computer simulations (NU-1000) also suggest that CO_2 binding sites lie close to the Zr_6 nodes and in the vicinity of the perfluoroalkyl groups, although no specific $CF_2\cdots CO_2$ interactions are invoked.[42]

Unlike the aforementioned highly porous fluorinated MOFs, however, the adsorption of CO_2 in AgCPs **1**-**5** more closely resembles the dissolution of CO_2 in perfluoroalkane solvents. The high CO_2 solubility in perfluoroalkanes[45-48] and the corresponding high solubility of small fluoroalkanes in liquid or supercritical CO_2[49-52] is well established. Indeed, the CO_2-fluoroalkyl attractive interaction has been subject of a number of experimental[31,53] and computational[54-56] studies, although the precise nature of the interaction remains an area of discussion.[31] This miscibility for CO_2 (and similarly for O_2 gas) has led to perfluoroalkyl groups being proposed as gas carriers in "artificial blood"[57,58] and for use in extracting CO_2 from waste streams.[59] The dissolution of CO_2 gas in highly fluorinated glassy polymers, which like AgCPs **1**-**5** have non-porous structures, has also been studied,[60-62] although their amorphous nature precludes accurate structural investigation of CO_2 inclusion sites. To the best of our knowledge, the present study provides the first example of crystal structures containing CO_2 molecules interacting with perfluoro*alkyl* chains in which the interactions with CO_2 are well defined. The structural insight provided therefore should also be of value to further investigations of fluorinated polymers in CO_2 adsorption and separation applications.

It seems reasonable to attribute the gating behaviour of the present materials during CO_2 adsorption to the need to overcome dispersion forces between the interdigitated perfluoroalkyl chains, which require greater CO_2 pressures to overcome greater dispersion forces between the longer chains but can lead to greater overall adsorption capacity. These assertions are supported by such dispersion forces between perfluoroalkyl chains giving rise to the monotonic trend in melting points and boiling points of perfluoroalkanes and -alkenes.[63] The ability to adjust the gating pressure and adsorption capacity by adjustment of the perfluoroalkyl chain length in this isoreticular series of AgCPs suggests a platform for tuning adsorption properties in these or related materials. Rational control of the pressure threshold in such Type F-III or F-IV (stepped) isotherms is extremely rare, but highly desirable in designing new materials for gas separation.[11,14]

The behaviour of AgCP **5** will require further investigation as PXRD studies suggest a gate pressure beyond the experimental limitations of our gravimetric adsorption studies is required to enable a larger CO_2 uptake, although very small uptakes were determined within the lower accessible pressure range ($p(CO_2) < 20$ bar at 273 K). The nature of the hystereses observed, most notably for **2** and **4**, is also an area in which further investigation would be informative.

Turning now to the potential for separation of CO_2 from CH_4, it is pertinent to note that gas solubility in liquids and polymers can be estimated based on the gas condensability (measured as critical temperature, normal boiling point or Lennard-Jones force constant) without accounting for specific interactions between solvent and solute.[64-66] The interactions between the guest molecule and the matrix in which it is dissolving, however, can either increase or suppress the gas solubility relative to that expected from correlation with the aforementioned physical properties. For example, perfluorinated gases, such as CF_4, C_2F_6 and C_3F_8, have a much lower solubility in hydrocarbon-based polymers like poly(dimethylsiloxane), PDMS, or low-density polyethylene, LDPE, than is predicted based on the solubility of light gases (e.g. N_2, O_2) and hydrocarbons. This reduced solubility has been attributed to the unfavourable interactions between perfluoroalkanes and alkanes,[62,66-68] which are immiscible as liquids. The same effect is found in the solutions of small hydrocarbon gases in perfluorocarbon media, where a reduction in solubility is found compared with the solubility in analogous hydrocarbon media.[69]

Large free-volume fluoropolymers have rather low CO_2/CH_4 selectivities.[20,70] In contrast, lower free-volume fluoropolymers exhibit greater CO_2/CH_4 selectivity due to the size-sieving ability and the increased unfavourable interactions between the fluorinated polymer framework and the CH_4 gas. The high selectivity of CO_2 over CH_4 exhibited by the highly fluorinated AgCPs in the present study is consistent with such a description of dissolution behaviour, but has permitted crystallographic identification of the CO_2 binding sites within the mobile perfluoroalkyl regions of the crystals. To the best of our knowledge, this is the first only example of such a CO_2 "dissolution" process occurring in a nonporous crystalline solid.

CONCLUSIONS

CO_2 sorption has been demonstrated by a family of highly fluorinated silver coordination polymers (AgCPs) **1-5** despite the absence of pores or channels in the crystal structures and contrasts with adsorption by highly porous fluorinated MOFs (*vide supra*), in which there has been considerable interest.[41] Gas uptake in **1-5** proceeds through a gate opening mechanism, resulting in Type F-III or F-IV CO_2 adsorption isotherms, in which the gas pressure threshold depends directly on the length of the perfluorocarboxylate chains that interdigitate to form perfluoroalkyl layers within the crystals. Gravimetric gas adsorption studies are complemented by *in situ* PXRD and SCXRD studies to provide structural and mechanistic insight into the sorption process.

Gas adsorption by nonporous crystals,[71-75] perhaps better described as crystals with latent porosity,[76] is known, but has received limited investigation compared to that in permanently porous materials. Gas transport in solids with latent porosity requires molecular mobility to aid transport. This is accomplished in the AgCPs by torsional flexibility of the perfluoroalkyl chains and flexibility along the coordination polymer backbone facilitated by non-directional coordination demands of the Ag(I) centres, enabling a process akin to dissolution of CO_2 in perfluoroalkane solvents or perfluorocarbon polymers. SCXRD studies reveal the location of the CO_2 molecule binding sites and identify interactions between CO_2 molecules, with the single-bridge aromatic TMP ligands and prominently with the perfluoroalkyl chains via $C{-}F^{\delta-}\cdots C^{\delta+}$ interactions.

Separation of CO_2 from CH_4 in gas mixtures with high selectivity has been demonstrated and is reinforced by single-component CH_4 adsorption studies that result in no significant uptake (Type III isotherms) nor volume increase in complementary diffraction studies. These relatively densely packed, but latently porous, materials suggest that perfluoroalkyl regions may be suitable to exploit for gas separations including tunability of gated sorption. The approach in this study has used complementary techniques to provide valuable insight into the nature of the sorption phenomena and has relevance beyond crystalline materials. It is hoped this will spur interest in similar new approaches to gas sorption/separation.

Supporting Information.

All relevant data are available from the authors, and/or are included with the manuscript Supplementary Information. The crystal structures of **1-MeOH, 1**(**1**$_A^{HT}$, **1**$_A^{LT}$, **1**$_B^{HT}$ and **1**$_B^{LT}$), **1**$_A^{CO2}$ (10 bar, 252 and 235K), **2-EtOH, 2** (**2**^{HT} and **2**^{LT}), **2**^{CO2} (10 bar, 215 and 200K), **3-EtOH, 3** (**3**^{HT} and **3**^{LT}), **3**$_A^{CO2}$ (10 bar, 230 and 215K), **3**$_B^{CO2}$, **4-MeOH, 4, 4**^{CO2}, **5-MeOH, 5** and **5**^{CO2} are available free of charge from the Cambridge Crystallographic Data Centre under reference numbers CCDC 654183, 1044595, 1044596, 1044597, 2329006-2329039.

AUTHOR INFORMATION

Corresponding Author

*vitorica@ugr.es

*lee.brammer@sheffield.ac.uk

Present Addresses

†Departamento de Química Inorgánica, Facultad de Ciencias, Universidad de Granada. Av. Fuente Nueva, 18070, Granada, Spain.

‡ Johnson Matthey Process Technologies, Inc., Savannah, GA 31408, USA.

Author Contributions

The manuscript was written through contributions of all authors. All authors have given approval to the final version of the manuscript. LB and IJVY conceived the project. IJVY synthesized the coordination polymers. IJVY, LB, MRW and SPT collected the XRD data and IJVY analysed the XRD data. AF measured and analysed the CO_2 isotherms. IJVY, MQ, SM and SM designed and built the gas cell/rig instrumentation used in the measurements at University of Manchester and described fully in the SI (Section S2).

Funding Sources

We thank EPSRC for funding via grant EP/F02195X/1 and a doctoral prize fellowship for IJVY and University of Manchester for funding.

Notes

The authors declare no competing financial interests.

ACKNOWLEDGMENTS

We are grateful to the Diamond Light Source for access to the Beamlines I11 and I19, and ESRF for access to beamline ID31 (currently ID22). We acknowledge the support of The University of Manchester X-ray diffraction service members and are grateful to The University of Manchester mechanical and electronic workshops for their assistance in the construction of the gas cell/rig instrumentation.

ABBREVIATIONS

AgCPs – silver coordination polymers; TMP – 2,3,5,6-tetramethylpyrazine.

1-MeOH - $[Ag_4(O_2C(CF_2)_2CF_3)_4(TMP)_3(MeOH)_2]$;

1 - $[Ag_4(O_2C(CF_2)_2CF_3)_4(TMP)_3]$;

1^{CO2} - $[Ag_4(O_2C(CF_2)_2CF_3)_4(TMP)_3]\cdot xCO_2$;

2-EtOH - $[Ag_4(O_2C(CF_2)_3CF_3)_4(TMP)_3(EtOH)_2]$;

2 - $[Ag_4(O_2C(CF_2)_3CF_3)_4(TMP)_3]$;

2^{CO2} - $[Ag_4(O_2C(CF_2)_3CF_3)_4(TMP)_3]\cdot xCO_2$;

3-EtOH - $[Ag_4(O_2C(CF_2)_4CF_3)_4(TMP)_3(EtOH)_2]$;

3 $[Ag_4(O_2C(CF_2)_4CF_3)_4(TMP)_3]$;

3^{CO2} - $[Ag_4(O_2C(CF_2)_4CF_3)_4(TMP)_3]\cdot xCO_2$;

4-MeOH - $[Ag_4(O_2C(CF_2)_5CF_3)_4(TMP)_3(MeOH)_2]$;

4 - $[Ag_4(O_2C(CF_2)_5CF_3)_4(TMP)_3]$;

4^{CO2} - $[Ag_4(O_2C(CF_2)_5CF_3)_4(TMP)_3]\cdot xCO_2$;

5-MeOH - $[Ag_4(O_2C(CF_2)_6CF_3)_4(TMP)_3(MeOH)_2]$;

5 - $[Ag_4(O_2C(CF_2)_5CF_3)_6(TMP)_3]$;

5^{CO2} - $[Ag_4(O_2C(CF_2)_6CF_3)_4(TMP)_3]_n\cdot xCO_2$;

REFERENCES

(1) Zhou, H.-C.; Kitagawa, S. Metal-Organic Frameworks (MOFs). *Chem. Soc. Rev.* **2014**, *43*, 5415−5418.

(2) Morris, R. E.; Wheatley P. S. Gas Storage in Nanoporous Materials. *Angew. Chem. Int. Ed.* **2008**, *47*, 4966–4981.

(3) Adil, K.; Belmabkhout, Y.; Pillai, R. S.; Cadiau, R. S.; Bhatt, P. M.; Assen, A. H.; Maurin G.; Eddaoudi, M. Gas/vapour separation using ultra-microporous metal–organic frameworks: insights into the structure/separation relationship. *Chem. Soc. Rev*. **2017**, *46*, 3402–3430.

(4) Sholl, D. S.; Lively, R. P. Seven chemical separations to change the world. *Nature* **2016**, *532*, 435–437.

(5) Kitagawa, S. Porous Materials and the Age of Gas. *Angew. Chem., Int. Ed.* **2015**, *54*, 10686–10687.

(6) Rangnekar, N.; Mittal, N.; Elyassi, B.; Caro, J.; Tsapatsis, M. Zeolite membranes – a review and comparison with MOFs. *Chem. Soc. Rev.* **2015**, *44*, 7128–7154.

(7) Gozalez-Garcia, P.; Activated carbon from lignocellulosics precursors: A review of the synthesis methods, characterization techniques and applications, *Renew Sust Energy Rev*. **2018**, *82*, 1393–1414.

(8) Ding, S.-Y.; Wang, W. Covalent organic frameworks (COFs): from design to applications. *Chem. Soc. Rev*. **2013**, *42*, 548-568.

(9) Zhang, X.; Chen, Z.; Liu, X.; Hanna, S. L.; Wang, X.; Taheri-Ledari, R.; Maleki, A.; Li, P.; Farha, O. K. A historical overview of the activation and porosity of metal–organic frameworks. *Chem. Soc. Rev.*, **2020**, *49*, 7406–7427.

(10) Horike, S.; Shimomura, S.; Kitagawa, S. Soft porous crystals. *Nat. Chem*. **2009**, *1*, 695–704.

(11) Nikolayenko, V. I.; Castell, D. C.; Sensharma, D.; Shivanna, M.; Loots, L.; Forrest, K. A.; Solanilla-Salinas, C. J.; Otake, K.-I.; Kitagawa, S.; Barbour, L. J.; Space, B.; Zaworotko, M. J. Reversible transformations between the non-porous phases of a flexible coordination network enabled by transient porosity. *Nat. Chem.* **2023**, *15*, 542–549.

(12) Simon, C. M.; Kim, J.; Gomez-Gualdron, D. A.; Camp, J. S.; Chung, Y. G.; Martin, R. L.; Mercado, R.; Deem, M. W.; Gunter, D.; Haranczyk, M.; Sholl, D. S.; Snurr, R. Q.; Smit, B. The materials genome in action: identifying the performance limits for methane storage. *Energy Environ. Sci.* **2015**, *8*, 1190–1199.

(13) Yang, Q.-Y.; Lama, P.; Sen, S.; Lusi, M.; Chen, K.-J.; Gao, W.-Y.; Shivanna, M.; Pham, T.; Hosono, N.; Kusaka, S.; Perry IV, J. J.; Ma, S.; Space, B.; Barbour, L. J.; Kitagawa, S.; Zaworotko, M. J. Reversible Switching between Highly Porous and Nonporous Phases of an Interpenetrated Diamondoid Coordination Network That Exhibits Gate-Opening at Methane Storage Pressures. *Angew. Chem. Int. Ed.* **2018**, *57*, 5684-5689.

(14) Wang, S.-Q.; Mukherjee, S.; Zaworotko, M. J. Spiers Memorial Lecture: Coordination networks that switch between nonporous and porous structures: an emerging class of soft porous crystals. *Faraday Discuss.* **2021**, *231*, 9–50.

(15) Li, J.-R.; Sculley, J.; Zhou, H.-C. Metal–Organic Frameworks for Separations. *Chem. Rev.* **2012**, *112*, 2, 869–932.

(16) Libri, S.; Mahler, M.; Mínguez Espallargas, G.; Singh, D. C. N. G.; Soleimannejad, J.; Adams, H.; Burgard, M. D.; Rath, N. P.; Brunelli, M.; Brammer, L. Ligand Substitution within Nonporous Crystals of a Coordination Polymer: Elimination from and Insertion into Ag-O Bonds by Alcohol Molecules in a Solid–Vapor Reaction. *Angew. Chem. Int. Ed.* **2008**, *47*, 1693–697.

(17) Vitórica-Yrezábal, I. J.; Mínguez Espallargas, G.; Soleimannejad, J.; Florence, A. J.; Fletcher, A. J.; Brammer, L. Chemical transformations of a crystalline coordination polymer: a multi-stage solid–vapour reaction manifold. *Chem. Sci*. **2013**, *4*, 696–708.

(18) Vitórica-Yrezábal, I. J.; Libri, S.; Loader, J. R.; Mínguez Espallargas, G.; Hippler, M.; Fletcher, A. J.; Thompson, S. P.; Warren, J. E.; Musumeci, D.; Ward, M. D.; Brammer, L. Coordination Polymer Flexibility Leads to Polymorphism and Enables a Crystalline Solid–Vapour Reaction: A Multi-technique Mechanistic Study. *Chem. Eur. J.* **2015**, *21*, 8799–8811.

(19) Perfluorocarbon liquids exhibit higher gas solubilities than their hydrocarbon analogues as a consequence of poorer molecular-scale packing.[20]

(20) Alentiev, Y.; Shantarovich, V. P.; Merkel, T. C.; Bondar, V. I.; Freeman, B. D.; Yampolskii, Y. P. Gas and vapor sorption, permeation, and diffusion in glassy amorphous Teflon AF1600. *Macromolecules* **2002**, *35*, 9513–9522.

(21) A. H. Hill, A new gas system for automated in situ powder diffraction studies at the European Synchrotron Radiation Facility, *J. Appl. Cryst.* **2013**, *46*, 570–572.

(22) Pawley, G. S., Unit-cell refinement from powder diffraction scans, *J. Appl. Crystallogr.*, **1981**, *14*, 357–361.

(23) CO_2 adsorption estimates are based upon CO_2 molecular volumes of 30.61 $Å^3$ (estimated by Gavazzotti[24]) and 38.3 $Å^3$ (estimated by van Heerden and Barbour[25]) as lower and upper bounds, respectively, and assume a 50% occupancy by CO_2 of the additional volume available.[25]

(24) Gavezzotti, A. The Calculation of Molecular Volumes and the Use of Volume Analysis in the Investigation of Structured Media and of Solid-State Organic Reactivity. *J. Am. Chem. Soc.* **1983**, *105*, 5220–5225.

(25) van Heerden, D. P.; Barbour, L. J. Guest-occupiable space in the crystalline solid state: a simple rule-of-thumb for predicting occupancy. *Chem. Soc. Rev.* **2021**, *50*, 735–749.

(26) Nowell, H.; Barnett, S. A.; Christensen, K. E.; Teat, S. J.; Allan, D. R. I19, the small-molecule single-crystal diffraction beamline at Diamond Light Source. *J Synchrotron Radiat*. **2012**, *19*, 435–441.

(27) Lee, H. M.; Youn, I. S.; Saleh, M.; Lee, J. W.; Kim, K. S. Interactions of CO_2 with various functional molecules. *Phys. Chem. Chem. Phys.* **2015**, *17*, 10925–10933

(28) Schottel, B. L.; Chifotides, H. T.; Dunbar, K. R. Anion-π interactions. *Chem. Soc. Rev*., **2008**, *37*, 68–83.

(29) Allen, F. H.; Baalham, C. A.; Lommerse, J. P. M.; Raithby, P. R. Carbonyl-Carbonyl Interactions can be Competitive with Hydrogen Bonds. *Acta Crystallogr.* **1998**, *B54*, 320−329.

(30) Lei, L.; da Silva, I.; Kolokolov, D. I.; Han, X.; Li, J.; Smith, G.; Cheng, Y.; Daemen, L. L.; Morris, C. G.; Godrey, H. G. W.; Jacques, N. M.; Zhang, X.; Manuel, P.; Frogley, M. D.; Murray, C. A.; Ramirez-Cuesta, A. J. Cinque, G.; Tang, C. C.; Stepanov, A. G.; Yang, S. Schröder, M. Post-synthetic modulation of the charge distribution in a metal–organic framework for optimal binding of carbon dioxide and sulfur dioxide. *Chem. Sci.* **2019,** *10*, 1472−1482.

(31) Costa Gomes, M. F.; Pádua, A. A. H. Interactions of Carbon Dioxide with Liquid Fluorocarbons, *J. Phys. Chem. B* **2003**, *107*, 50, 14020–14024

(32) Vitórica-Yrezábal, I. J.; Florin Sava, D.; Timco, G. A.; Brown, M. S.; Savage, M.; Godfrey, H. G. W.; Moreau, F. Schröder, M.; Siperstein, F.; Brammer, L.; Yang, S.; Attfield, M. P.; McDouall, J. J. W.; Winpenny, R. E. P. Binding CO_2 by a Cr_8 Metallacrown. *Angew. Chem. Int. Ed.* **2017**, *56*, 5527−5530.

(33) Nugent, P.; Belmabkhout, Y.; Burd, S. D.; Cairns, A. J.; Luebke, R.; Forrest, K.; Pham, T.; Ma, S.; Space, B.; Wojtas, L.; Eddaoudi, M.; Zaworotko, M. J. Porous materials with optimal adsorption thermodynamics and kinetics for CO2 separation. *Nature* **2013**, *495*, 80−84.

(34) Nugent, P.; Rhodus, V.; Pham, T.; Tudor, B.; Forrest, K.; Wojtas, L.; Space, B.; Zaworotko, M. Enhancement of CO2 selectivity in a pillared pcu MOM platform through pillar substitution. *Chem. Commun.* **2013**, *49*, 1606−1608.

(35) CO_2 gas sorption has been studied in MOFs containing fluorinated ligands,[36-44] but unlike the present study such materials have permanent porosity and thereby provide a direct pathway for gas sorption

(36) Pachfule, P.; Chen, Y.; Jiang, J.; Banerjee, R. Fluorinated Metal–Organic Frameworks: Advantageous for Higher H_2 and CO_2 Adsorption or Not? *Chem. Eur. J*. **2012**, *18*, 688–694.

(37) Seo, J.; Bonneau, C.; Matsuda, R.; Takata, M.; Kitagawa, S. Soft Secondary Building Unit: Dynamic Bond Rearrangement on Multinuclear Core of Porous Coordination Polymers in Gas Media. *J. Am. Chem. Soc.* **2011**, *133*, 23, 9005–9013.

(38) Kosaka, W.; Liu, Z.; Zhang, J.; Sato, Y.; Hori, A.; Matsuda, R.; Kitagawa, S.; Miyasaka, H. Gas-responsive porous magnet distinguishes the electron spin of molecular oxygen. *Nat. Commun*. **2018**, *9*, 5420.

(39) Zhang, J.; Kosaka, W.; Kitagawa, Y.; Miyasaka, H. A metal-organic framework that exhibits CO_2-induced transitions between paramagnetism and ferrimagnetism. *Nat. Chem*. **2021**, *13*, 191–199.

(40) Dou, C.; Kosaka, W.; Miyasaka, H. Gate-open-type Sorption in a Zigzag Paddlewheel Ru Dimer Chain Compound with a Phenylenediamine Linker Instructed by a Preliminary Structural Change of Desolvation. *Chem. Lett.* **2017**, *46*, 1288–1291.

(41) Amooghin, A. E.; Sanaeepur, H.; Luque, R.; Garcia, H.; Chen, B. Fluorinated metal–organic frameworks for gas separation. *Chem. Soc. Rev.* **2022**, *51*, 7427−7508.

(42) Deria, P.; Mondloch, J. E.; Tylianakis, E.; Ghosh, P.; Bury, W.; Snurr, R. Q.; Hupp, J. T.; Farha, O. K. Perfluoroalkane Functionalization of NU-1000 via Solvent-Assisted Ligand Incorporation: Synthesis and CO_2 Adsorption Studies. *J. Am. Chem. Soc*. **2013**, *135*, 16801−16804.

(43) Drache, F.; Bon, V.; Senkovska, I.; Marschelke, C.; Synytska, A.; Kaskel, S. Postsynthetic Inner-Surface Functionalization of the Highly Stable Zirconium-Based Metal−Organic Framework DUT-67. *Inorg. Chem.* **2016**, *55*, 7206−7213.

(44) Thür, R.; Van Velthoven, N.; Lemmens, V.; Bastin, M.; Smolders, S.; De Vos, D.; Vankelecom, I. F, J. Modulator-Mediated Functionalization of MOF-808 as a Platform Tool to Create High-Performance Mixed-Matrix Membranes. *ACS Appl. Mater. Interfaces* **2019**, *11*, 44792−44801.

(45) Dardin, A.; DeSimone, J. M.; Samulski, E. T. Fluorocarbons Dissolved in Supercritical Carbon Dioxide. NMR Evidence for Specific Solute−Solvent Interactions. *J. Phys. Chem. B* **1998**, *102*, 1775–1780.

(46) Yee, G. G.; Fulton, J. L.; Smith, R. D. Fourier Transform Infrared Spectroscopy of Molecular Interactions of Heptafluoro-1 -butanol or 1-Butanol In Supercritical Carbon Dioxide and Supercritical Ethane *J. Phys. Chem.* **1992**, *96*, 6172–6181.

(47) Yonker, C. R. Solution Dynamics of Perfluorobenzene, Benzene, and Perdeuteriobenzene in Carbon Dioxide as a Function of Pressure and Temperature, *J. Phys. Chem. A* **2000**, *104*, 685–691.

(48) Yonker, C. R.; Palmer, P. J. Investigation of CO_2/Fluorine Interactions through the Intermolecular Effects on the ^{1}H and ^{19}F Shielding of CH_3F and CHF_3 at Various Temperatures and Pressures, *J. Phys. Chem. A* **2001**, *105*, 308–314.

(49) Riess, J. G.; Le Blanc, M. Solubility and transport phenomena in perfluorochemicals relevant to blood substitution and other biomedical applications, *Pure Appl. Chem.* **1982**, *54*, 2383–2406.

(50) Iezzi, A.; Bendale, P.; Enick, R.; Turberg, M.; Brady, J. Gel formation in carbon dioxide-semifluorinated alkane mixtures and phase equilibria of a carbon dioxide-perfluorinated alkane mixture, *Fluid Phase Equilib.* **1989**, *52*, 307–317.

(51) Kho, Y. W.; Conrad, D. C.; Knutson, B. L. Phase equilibria and thermophysical properties of carbon dioxide-expanded fluorinated solvents, *Fluid Phase Equilib.* **2003**, *206*, 179–193.

(52) Lazzaroni, M. J.; Bush, D.; Brown, J. S.; Eckert, C. A. High-Pressure Vapor−Liquid Equilbria of Some Carbon Dioxide + Organic Binary Systems, *J. Chem. Eng. Data*, **2005**, *50*, 60–65.

(53) Raveendran, P.; Wallen, S. L. Exploring CO_2-Philicity: Effects of Stepwise Fluorination, *J. Phys. Chem. B*, **2003** ,*107* ,1473–1477.

(54) Diep, P.; Jordan, K. D.; Johnson, J. K.; Beckman, E. J. CO2−Fluorocarbon and CO2−Hydrocarbon Interactions from First-Principles Calculations, *J. Phys. Chem. A,* **1998**, *102*, 12, 2231–2236.

(55) Cece, A.; Jureller, S. H.; Kerschner, J. L.; Moschner, K. F. Molecular Modeling Approach for Contrasting the Interaction of Ethane and Hexafluoroethane with Carbon Dioxide*, J. Phys. Chem.,* **1996**, *100*, 18, 7435–7439.

(56) Dias, A. M. A.; Carrier, H.; Daridon, J. L.; Pàmies, J. C.; Vega, L. F.; Coutinho, J. A. P.; Marrucho, I. M. Vapor-Liquid Equilibrium of Carbon Dioxide-Perfluoroalkane Mixtures: Experimental Data and SAFT Modeling, *Ind. Eng. Chem. Res.*, **2006**, *45*, 2341-2350.

(57) Riess, J. G. Oxygen Carriers ("Blood Substitutes"). *Chem. Rev*. **2001**, *101*, 9, 2797–2920.

(58) Wasanathian, A; Peng, C.-A. Enhancement of micro algal growth by using perfluorocarbon as oxygen carrier. *Artificial Cells, Blood Substitutes Biotechnol.* **2001**, *29*, 47–55.

(59) Stallone, K. B.; Bonner, F. J. A low cost environmentally benign CO_2 based hydrometallurgical process. *Green Chem*., **2004**, *6,* 267–270.

(60) Bondar, V. I.; Freeman, B. D.; Yampolskii, Y. P. Sorption of Gases and Vapors in an Amorphous Glassy Perfluorodioxole Copolymer. *Macromolecules* **1999**, *32*, 6163–6171.

(61) Merkel, T. C.; Bondar, V. I.; Nagai, K.; Freeman, B. D.; Yampolskii, Y. P. Gas Sorption, Diffusion, and Permeation in Poly(2,2-bis(trifluoromethyl)-4,5-difluoro-1,3-dioxole-co-tetrafluoroethylene). *Macromolecules* **1999**, *32*, 8427–8440.

(62) Prabhakar, R. S.; De Angelis, M.-G.; Sarti, G. C.; Freeman, B. D.; Coughlin, M. C. Gas and Vapor Sorption, Permeation, and Diffusion in Poly(tetrafluoroethylene-co-perfluoromethyl vinyl ether), *Macromolecules* **2005**, *38*, 7043–7055.

(63) Anderson, H. H. Boiling Points and Boiling Point Numbers of Perfluoroalkanes and Perfluoroalkenes. *J. Chem. Eng. Data* **1965**, *2*, 156–159.

(64) Van Amerongen, G. J. Influence of structure of elastomers on their permeability to gases. *J. Polym. Sci.*, **1950**, *5*, 307–332.

(65) Korosy, F. Two rules concerning solubility of gases and crude data on solubility of krypton. *Trans. Faraday Soc.* **1937**, *33*, 416–425.

(66) Merkel, T. C.; Bondar, V. I.; Nagai, K.; Freeman, B. D.; Pinnau, I. Gas sorption, diffusion, and permeation in poly(dimethylsiloxane). *J. Polym. Sci., Part B: Polym. Phys.* **2000**, *38*, 415–434.

(67) Merkel, T. C.; Bondar, V.; Nagai, K.; Freeman, B. D. Hydrocarbon and Perfluorocarbon Gas Sorption in Poly(dimethylsiloxane), Poly(1-trimethylsilyl-1-propyne), and Copolymers of Tetrafluoroethylene and 2,2-Bis(trifluoromethyl)-4,5- difluoro-1,3-dioxole. *Macromolecules* **1999**, *32*, 370–374.

(68) Kamiya, Y.; Naito, Y.; Terada, K.; Mizoguchi, K.; Tsuboi, A. Volumetric Properties and Interaction Parameters of Dissolved Gases in Poly(dimethylsiloxane) and Polyethylene. *Macromolecules* **2000**, *33*, 3111–3119.

(69) Scott, R. The Anomalous Behavior of Fluorocarbon Solutions. *J. Phys. Chem*. **1958**, *62*, 136–145.

(70) Prabhakar, R. S.; Freeman, B. D.; Roman, I. Gas and Vapor Sorption and Permeation in Poly(2,2,4-trifluoro-5-trifluoromethoxy-1,3-dioxole-co-tetrafluoroethylene). *Macromolecules* **2004**, *37*, 7688-7697.

(71) Albrecht, M; Lutz, M.; Spek, A. L.; van Koten, G. Organoplatinum crystals for gas-triggered switches. *Nature* **2000**, *406*, 970–974.

(72) Atwood, J. L.; Barbour, L. J.; Jerga, A. A New Type of Material for the Recovery of Hydrogen from Gas Mixtures. *Angew. Chem. Int. Ed.* **2004**, *43*, 2948–2950.

(73) Mínguez Espallargas, G.; Hippler, M.; Florence, A. J.; Fernandes, P.; van de Streek, J.; Brunelli, M.; David, W. I. F.; Shankland, K.; Brammer, L. Reversible Gas Uptake by a Nonporous Crystalline Solid Involving Multiple Changes in Covalent Bonding. *J. Am. Chem. Soc.* **2007**, *129*, 15606–15614.

(74) Huang, Z.; White, P. S.; Brookhart, M. Ligand exchanges and selective catalytic hydrogenation in molecular single crystals. *Nature* **2010**, *465*, 598–601.

(75) Pike, S. D.; Thompson, A. L.; Algarra, A. G.; Apperley, D. C.; Macgregor, S. A.; Weller, A. S. Synthesis and Characterization of a Rhodium(I) σ-Alkane Complex in the Solid State. *Science* **2012**, *337*, 1648–1651.

(76) Barbour, L. J. Crystal porosity and the burden of proof. *Chem. Commun.* **2006**, 1163–1168.